

## Supporting Information

### **Red Luminescent Helical Ribbons Based on Nonpolar Charge-Transfer Complex**

Jiacheng Zhang,<sup>a</sup> Lei Yao,<sup>a</sup> Wenju Li,<sup>a</sup> Yongyi Zhang,<sup>a</sup> Tao Jin,<sup>a</sup> Guan Wang,<sup>a</sup> Jing Zhang,<sup>\*a</sup> Jianfen Zhao<sup>\*b</sup>

**\*Jing Zhang** - <sup>a</sup>State Key Laboratory of Organic Electronics and Information Displays, Institute of Advanced Materials (IAM), Nanjing University of Posts & Telecommunications, 9 Wenyuan Road, Nanjing 210023, China;

*E-mail: iamjingzhang@njupt.edu.cn*

**\*Jianfen Zhao** - <sup>b</sup>Key Laboratory of Flexible Electronics (KLOFE) & Institute of Advanced Materials (IAM), Jiangsu National Synergetic Innovation Center for Advanced Materials (SICAM), Nanjing Tech University (Nanjing Tech), 30 South Puzhu Road, Nanjing 211816, China.

*E-mail: iamjfzhao@njtech.edu.cn*

## Table of Contents

<b>Experimental Procedures.....</b>	<b>3</b>
Materials.....	3
Crystals Growth and Structural Analysis.....	3
Growth of the ribbons and micro-helices on the Substrates .....	3
Measurements.....	3
Theoretical Calculation Details. ....	3
<b>Results and Discussion .....</b>	<b>4</b>
Fig. S1 OM images of DNF-DCAF ribbons prepared from high concentration solution.....	4
Fig. S2 OM images of DNF-DCAF micro-helices prepared from low concentration solution....	4
Fig. S3 SEM images of DNF-DCAF micro-helices.....	5
Fig. S4 OM images of DNF-DCAF microcrystals prepared from intermediate concentration solution.....	5
Fig. S5 Twisted DNF-DCAF crystals with different helical pitches obtained from different concentration solution.....	6
Fig. S6 Jablonski diagram of DNF-DCAF cocrystal.....	6
Fig. S7 OM and corresponding PL images of DNF-DCAF crystals with different morphologies.....	7
Fig. S8 PL spectra of DNF-DCAF crystals with different morphologies (thicknesses).....	7
Fig. S9 IR spectra of DCAF and DNF-DCAF cocrystal .....	8
Fig. S10 Energy level diagram for DNF, DCAF and DNF-DCAF cocrystal.....	8
Fig. S11 The dipole moments of one DA pair in DNF-DCAF cocrystal.....	8
Table S1 Crystal data and structure refinement for DNF-DCAF cocrystal.....	9
<b>References.....</b>	<b>9</b>

## Experimental Procedures

**Materials.** DNF and DCAF were purchased from Bide Pharmatech Co., Ltd. All of them were used directly as received without further Purification. All solvents were HPLC grade.

**Crystals Growth and Structural Analysis.** DNF-DCAF complexes were prepared by acetonitrile solution. First, dissolve the mixture of DNF and DCAF (molar ratio of 1:1) in acetonitrile to obtain a solution with a concentration of 1 mg/mL. After heating at 70 °C for 1 hour to ensure complete dissolution, the mixed solution was left in the air to slowly evaporate for three to four days, until the liquid completely disappeared and DNF-DCAF bulk cocrystals were finally found at the bottom of the bottle. Subsequently, the bulk cocrystals were filtered from the solution and dried in the air. The Bruker smart-1000-CCD diffractometer with graphite-monochromatic Mo  $K\alpha$  radiation ( $\lambda = 0.71073 \text{ \AA}$ ) was used to measure the crystal structures of DNF-DCAF single crystals. The X-ray crystallographic data were collected at low temperature of 193K. The structure was resolved by the direct method and refined by the full-matrix least-squares method on *F*<sup>2</sup> using the SHELXL-97 program.

**Growth of the ribbons and micro-helices on the Substrates.** In order to grow ribbons on the substrate, an acetonitrile solution (1 mg/mL) containing DNF and DCAF in a molar ratio of 1:1 was drop-cast onto the SiO<sub>2</sub>/Si substrate. As the solvent evaporates, ribbon crystallites were prepared on the substrate. When the concentration of acetonitrile was reduced to 0.3 mg/mL, micro-helices were obtained by the same method.

**Measurements.** The cocrystal nanostructures were characterized by optical microscopy (BX53, Olympus), UV–visible absorption spectrum (UV–vis spectra, LAMBDA 35), Scanning electron microscope (Bruker, S4800), Infrared Spectrometer (PE Spectrum Two). PXRD was measured on a D/max2500 with Cu  $K\alpha$  source ( $\kappa = 1.541 \text{ \AA}$ ).

**Theoretical Calculation Details.** The Vienna ab initio simulation package (VASP 5.4.4) and PEB functional were used to calculate the energy levels of the crystals.<sup>1-3</sup> ORCA software was used to calculate the dipole moments of DNF-DCAF, and the lattice constants and atomic positions of DNF-DCAF were optimized based on density functional theory (DFT). The reciprocal space was covered by a  $\Gamma$ - centered Monkhorst-Pack lattice of  $3 \times 3 \times 3$  *K*-points. The convergence criteria were set to  $10^{-5}$  eV for the SCF and  $-0.001 \text{ eV \AA}^{-1}$  for the geometry optimization.

## Results and Discussion

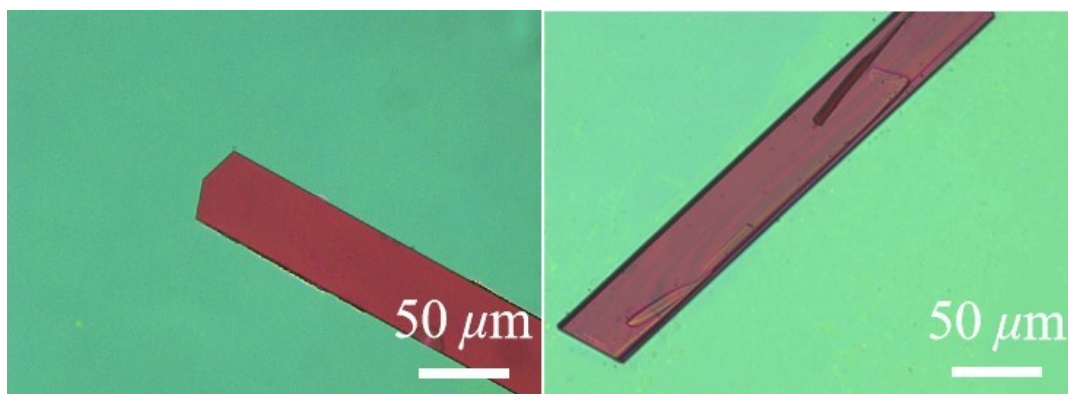


**Fig. S1** OM images of DNF-DCAF ribbons prepared from high concentration solution of  $\sim 1.0$  mg/mL.

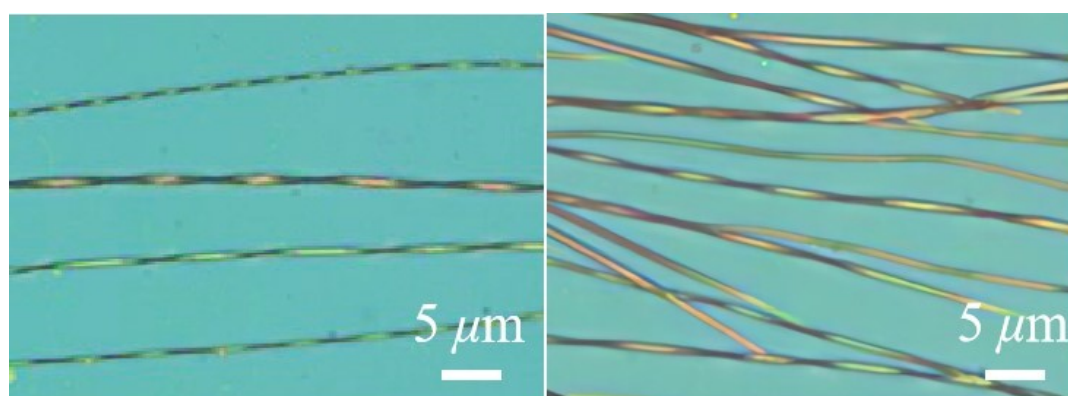


**Fig. S2** OM images of DNF-DCAF micro-helices prepared from low concentration of  $\sim 0.3$  mg/mL.

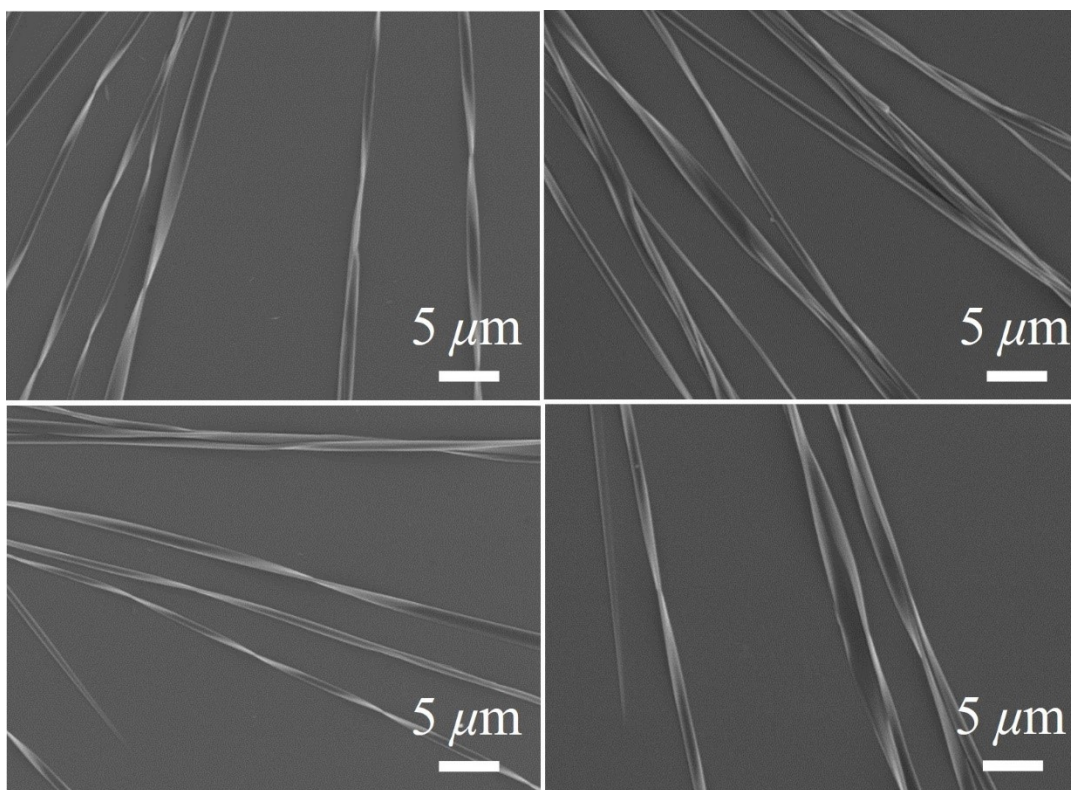


**Fig. S3** SEM images of DNF-DCAF micro-helices.

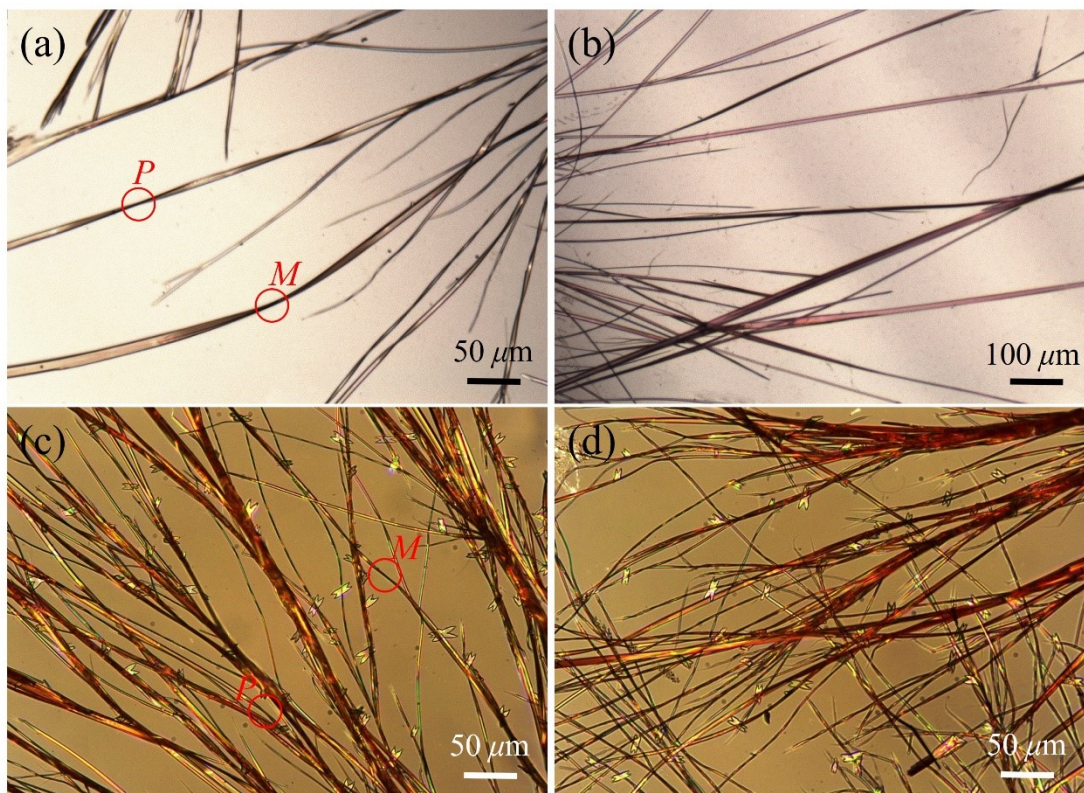


**Fig. S4** OM images of DNF-DCAF microcrystals prepared from different concentrations: (a, b) ~0.5 mg/mL and (c, d) ~0.7 mg/mL.

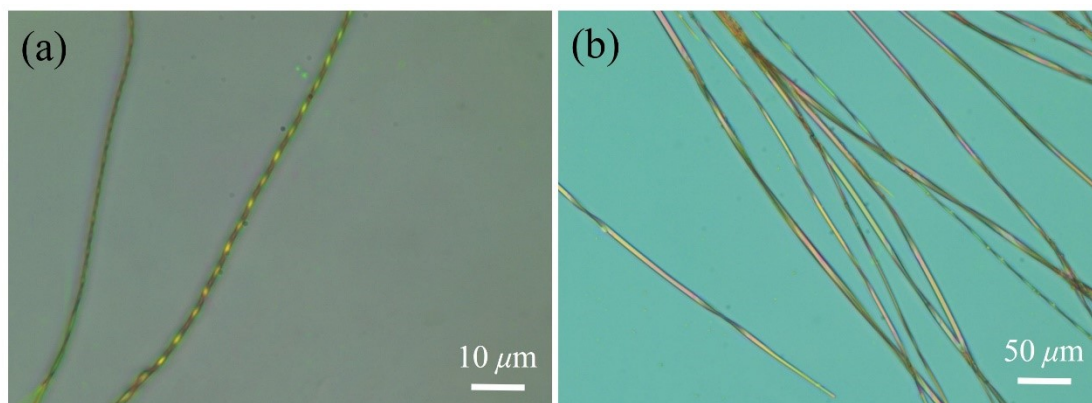


**Fig. S5** Twisted DNF-DCAF crystals with different helical pitches obtained from (a)  $\sim 0.1$  mg/mL and (b)  $\sim 0.5$  mg/mL solutions.

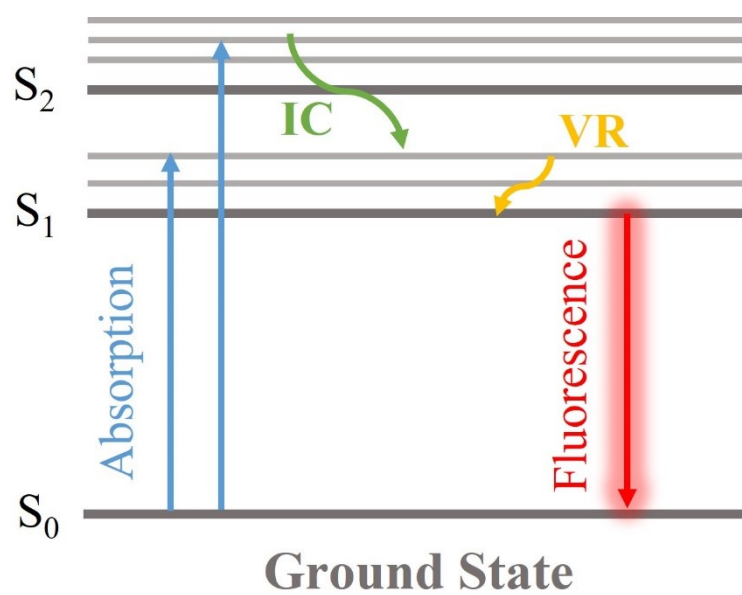


**Fig. S6** Jablonski diagram of DNF-DCAF cocrystal.

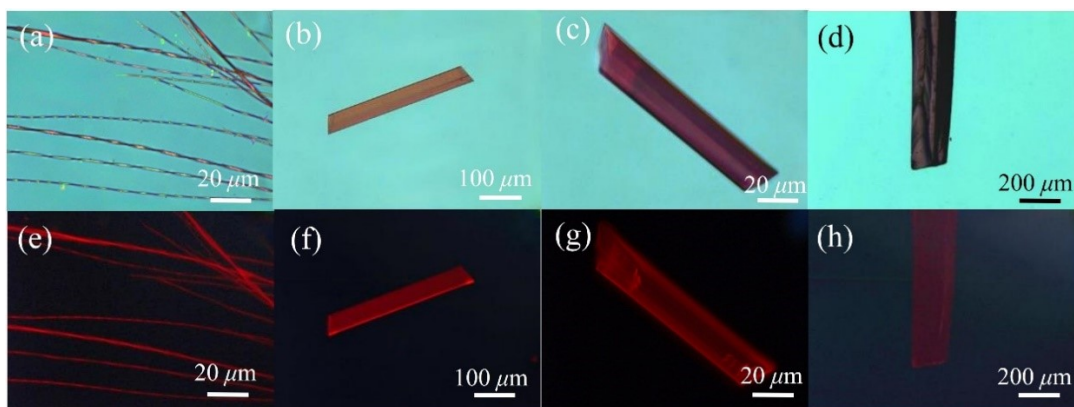


**Fig. S7** (a-d) OM and (e-h) corresponding PL images of DNF-DCAF crystals with different morphologies.

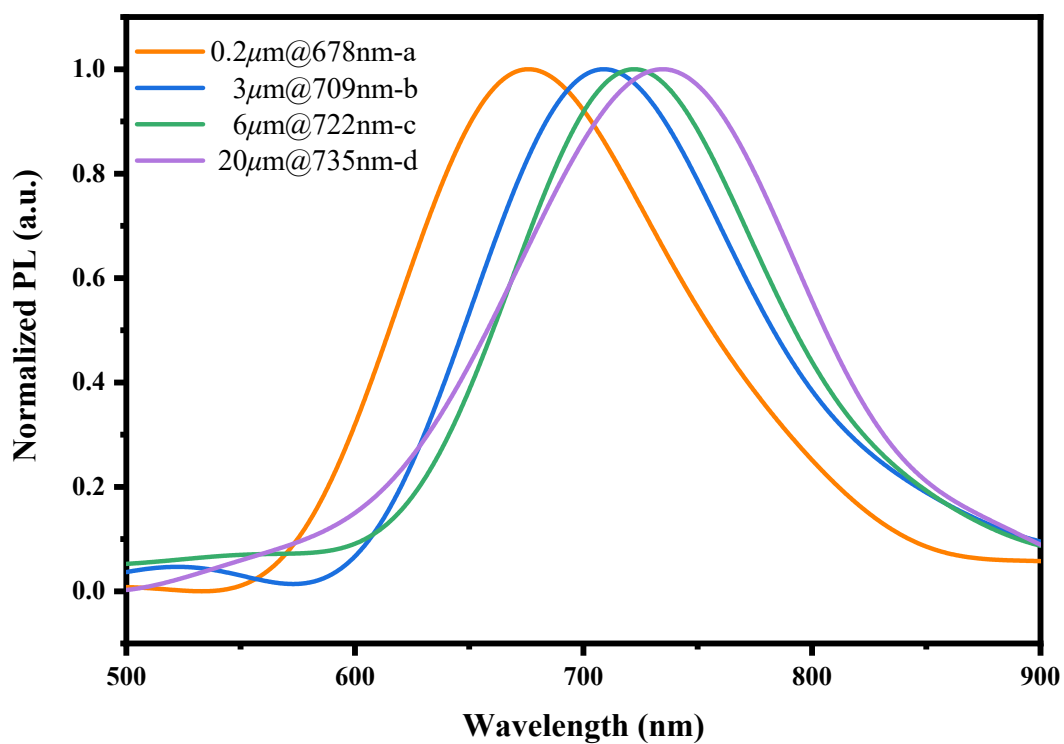


**Fig. S8** PL spectra of DNF-DCAF crystals with different morphologies (thicknesses).

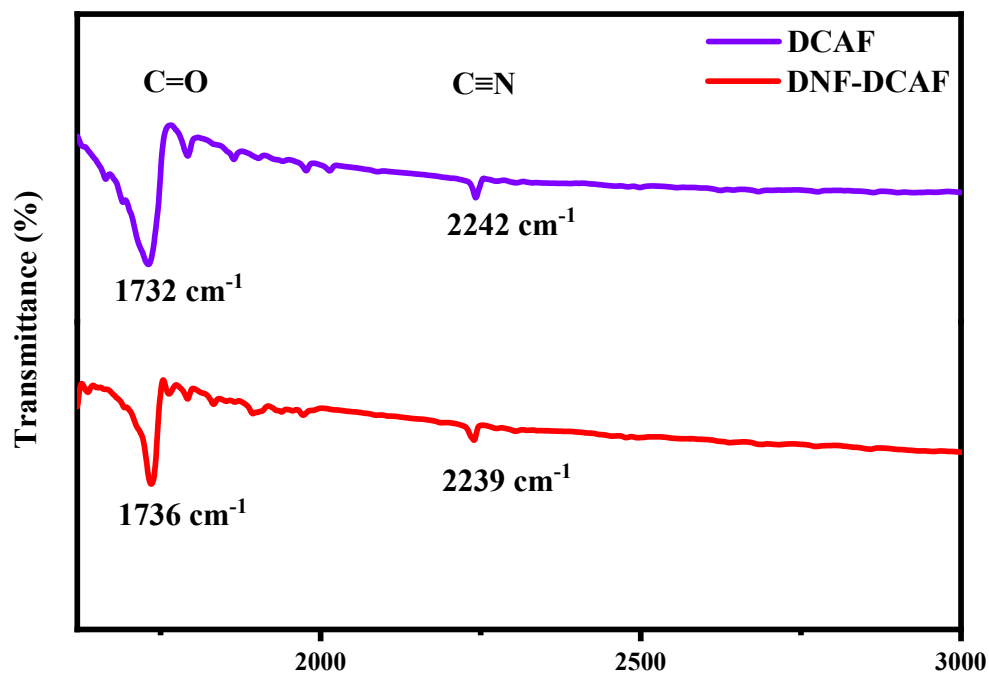


**Fig. S9** IR spectra of DCAF and DNF-DCAF cocrystal.

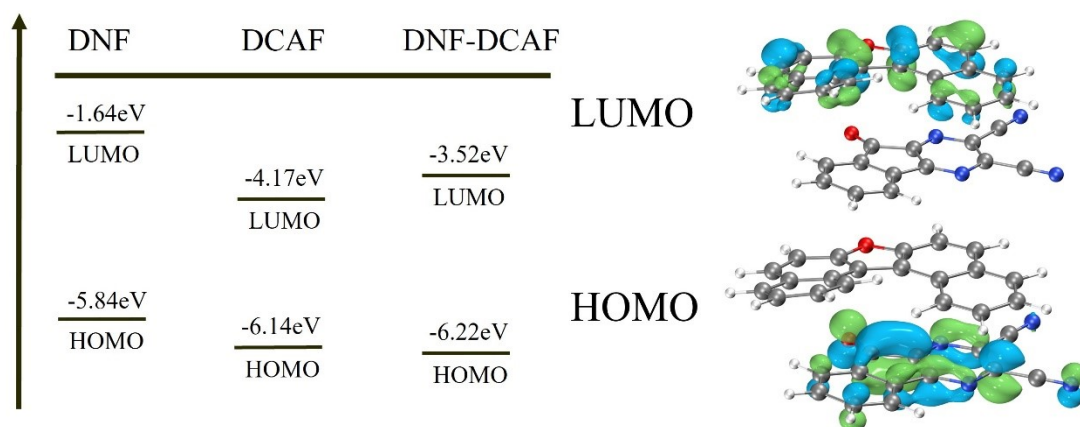


**Fig. S10** Energy level diagram for DNF, DCAF and DNF-DCAF cocrystal.

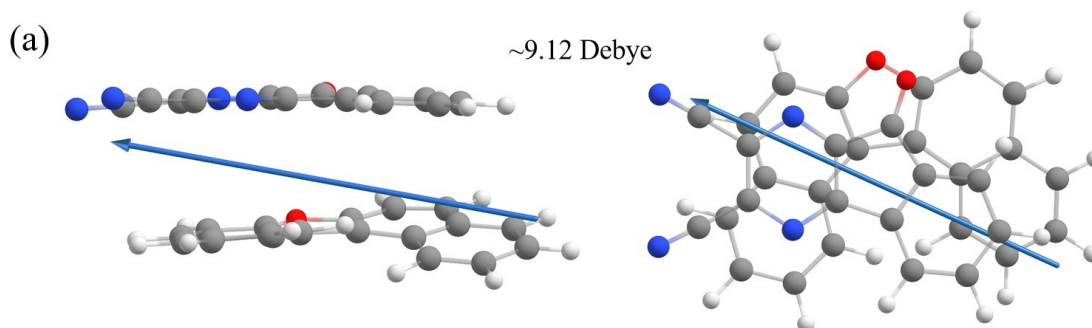


**Fig. S11** The dipole moments of one DA pair in DNF-DCAF cocrystal.



**Table S1** Crystal data and structure refinement for DNF-DCAF cocrystal.

	<b>DNF-DCAF</b>
Formula	C <sub>33</sub> H <sub>16</sub> N <sub>4</sub> O <sub>2</sub>
Formula weight	500.50
Temperature (K)	193
Wavelength (Å)	0.71073
Crystal system	Monoclinic
space group	<i>P</i> 2 <sub>1</sub> / <i>c</i>
<b>Unit cell dimensions</b>	
<i>a</i> (Å)	17.9169(19)
<i>b</i> (Å)	7.1865(6)
<i>c</i> (Å)	18.670(2)
<i>α</i> (°)	90
<i>β</i> (°)	103.464(4)
<i>γ</i> (°)	90
Volume (Å <sup>3</sup> )	2337.8(4)
Z	4
Absorption coefficient (mm <sup>-1</sup> )	0.732
<i>F</i> (000)	1032.0
Crystal size (mm)	0.15 × 0.13 × 0.12
θ range (°)	4.866 to 67.939
<b>Limiting indices</b>	-16 ≤ <i>h</i> ≤ 21 -8 ≤ <i>k</i> ≤ 7 -22 ≤ <i>l</i> ≤ 22
Reflections collected	13980
R(int)	0.0630
Absorption correction	Semi-empirical from equivalents
Refinement method	Full-matrix least-squares on <i>F</i> <sup>2</sup>
R [ <i>I</i> > 2σ( <i>I</i> )]	<i>R</i> <sub>1</sub> = 0.0491 <i>wR</i> <sub>2</sub> = 0.1210
R (all data)	<i>R</i> <sub>1</sub> = 0.0730 <i>wR</i> <sub>2</sub> = 0.1371
CCDC NO.	2340766

## References

- (1) P. E. Blöchl, *Phys. Rev. B*, 1994, **50**, 17953-17979.
- (2) G. Kresse, and J. Hafner, *J. Phys.: Condens. Matter*, 1994, **6**, 8245.
- (3) G. Kresse, and J. Furthmüller, *Comp. Mater. Sci.*, 1996, **6**, 11-50.